Supplementary Figure 1

A

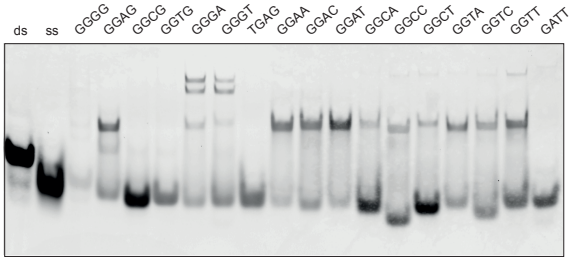

B

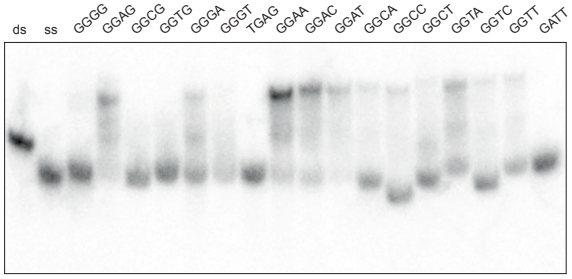

C

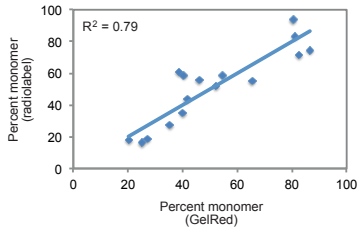

Supplementary Figure 1. Comparison of methods to visualize multimeric G-quadruplexes. (A) Native gel loaded with unlabeled DNA and stained with GelRed. (B) Native gel loaded with radiolabeled DNA and scanned using a Typhoon phosphorimager. (C) Comparison of the extent of monomer formation for unlabeled DNA stained with GelRed (x axis) and radiolabeled DNA (y axis). Experiments were typically performed at 10 μM G-quadruplex concentration in a buffer containing 200 mM KCl, 1 mM $MgCl_2$, and 20 mM HEPES pH 7.1.

Supplementary Figure 2

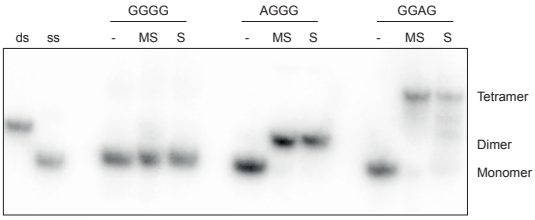

Supplementary Figure 2. Analysis of G-quadruplexes folded in mass spectrometry buffer on a native gel. Reactions were performed using a construct with a central GGGG tetrad and the sequence GGGTGGGAAGGGTGGGA, a construct with an AGGG mutation in the central tetrad of the reference construct and the sequence GAGTGGGAAGGGTGGGA, and a construct with a GGAG mutation in the central tetrad of the reference construct and the sequence GGGTGGGAAGAGTGGGA. Final conditions were 10 μM DNA concentration in a buffer containing either 20 mM HEPES pH 7.1 (lanes labeled “-“), 200 mM NH_4OAc pH 7 (lanes labeled “MS”), or 200 mM KCl, 1 mM $MgCl_2$, and 20 mM HEPES pH 7.1 (lanes labeled “S”).

Supplementary Figure 3

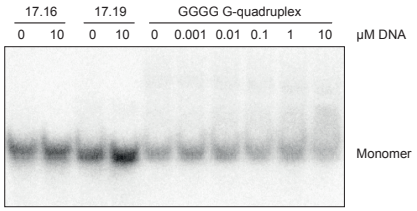

Supplementary Figure 3. Mobility of the reference construct on a native gel as a function of DNA concentration. 17.16 = a 17 nucleotide random sequence pool; 17.19 = a 17 nucleotide oligonucleotide with the sequence GACTGCCTCGTCACGAT; GGGG G-quadruplex = the reference G-quadruplex with a central GGGG tetrad and the sequence GGGTGGGAAGGGTGGGA. Final conditions were ≤ 500 pM radiolabeled DNA and 0-10 μM unlabeled DNA (indicated above each lane) in a buffer containing 200 mM KCl, 1 mM $MgCl_2$, and 20 mM HEPES pH 7.1.

Supplementary Figure 4

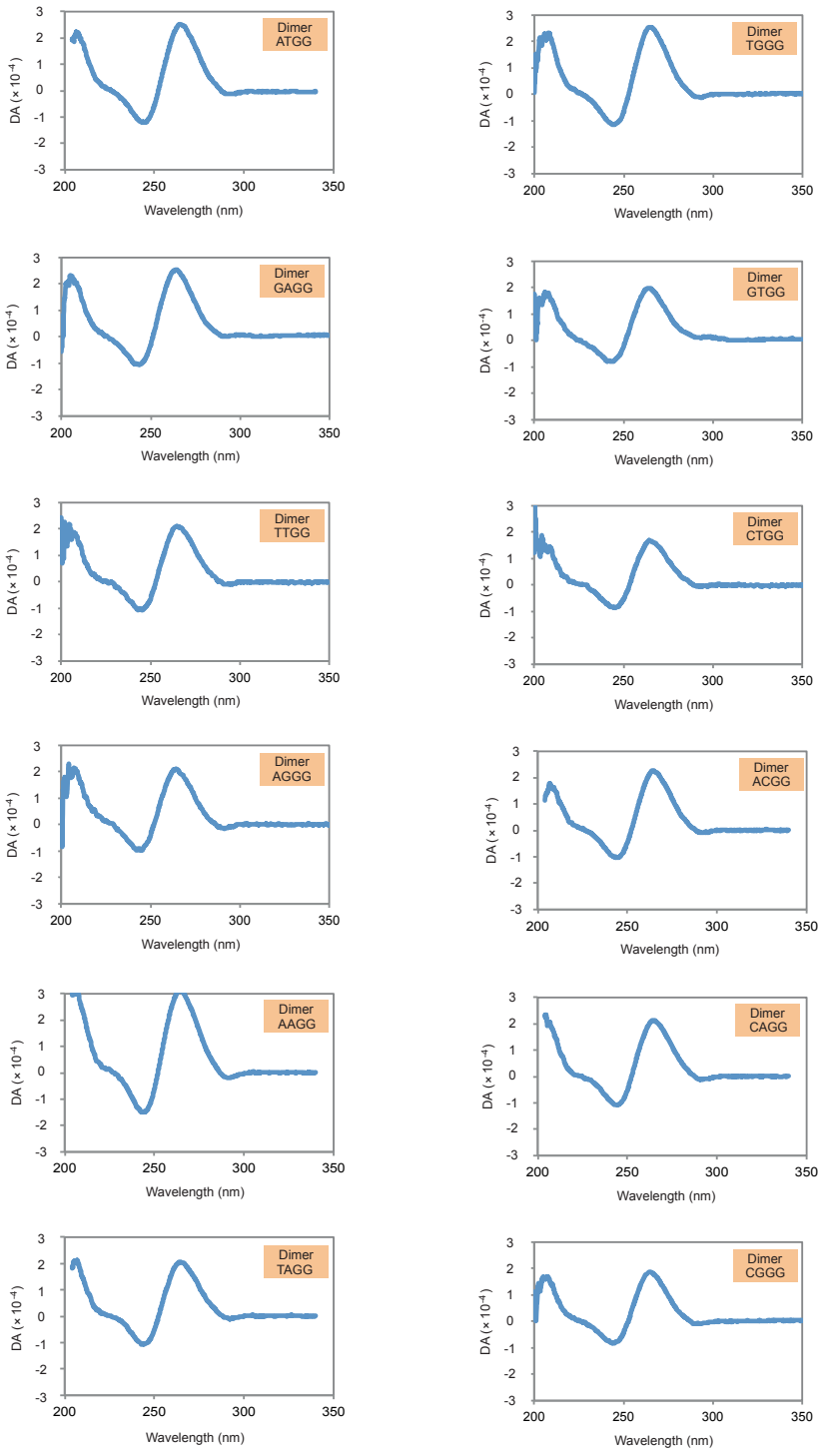

Supplementary Figure 4. Circular dichroism spectra of dimeric G-quadruplexes. Experiments were performed at 10 μM DNA concentration in a buffer containing 200 mM KCl, 1 mM $MgCl_2$, and 20 mM HEPES pH 7.1.

Supplementary Figure 5

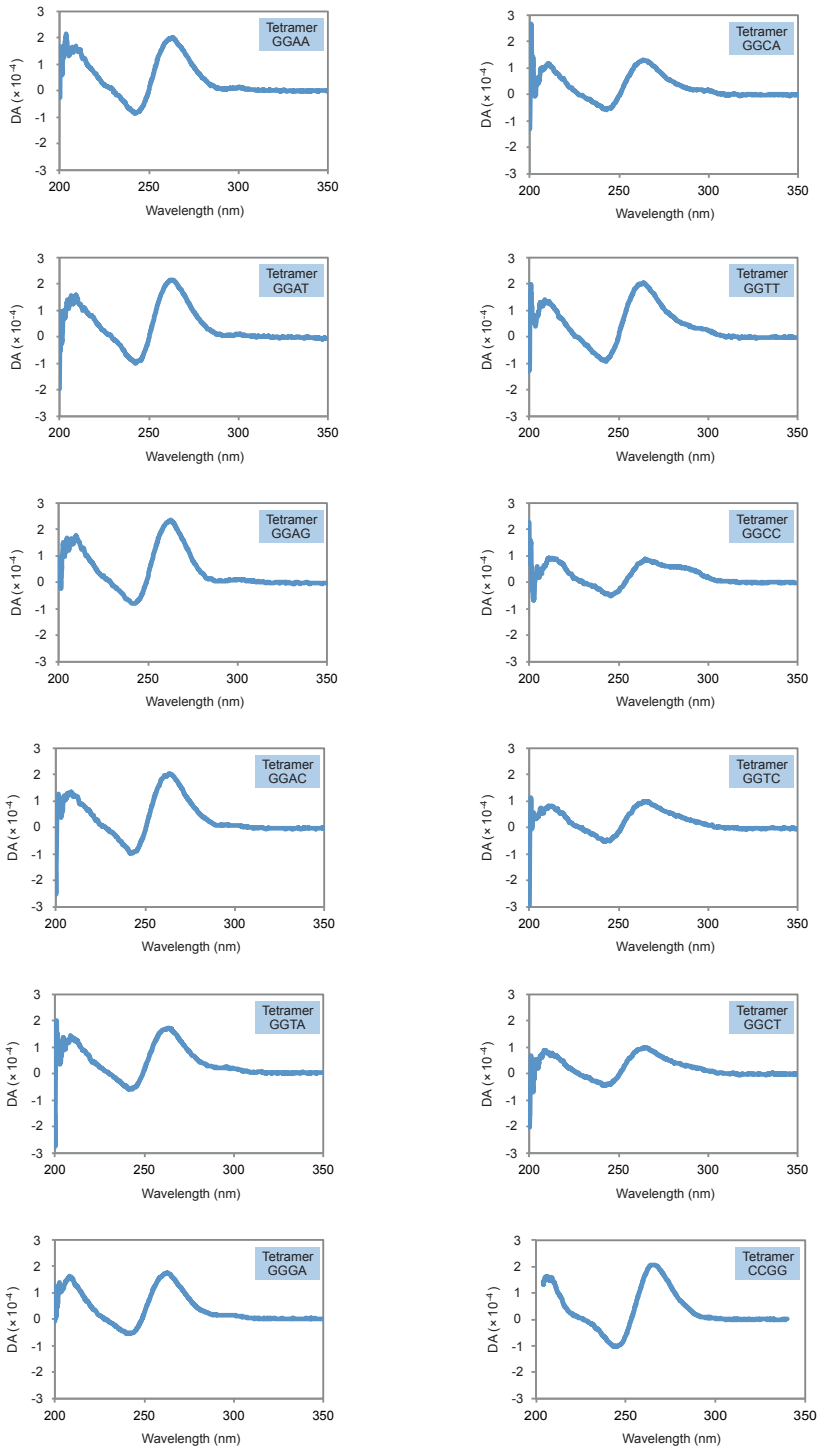

Supplementary Figure 5. Circular dichroism spectra of tetrameric G-quadruplexes. Experiments were performed at 10 μM DNA concentration in a buffer containing 200 mM KCl, 1 mM $MgCl_2$, and 20 mM HEPES pH 7.1.

Supplementary Figure 6

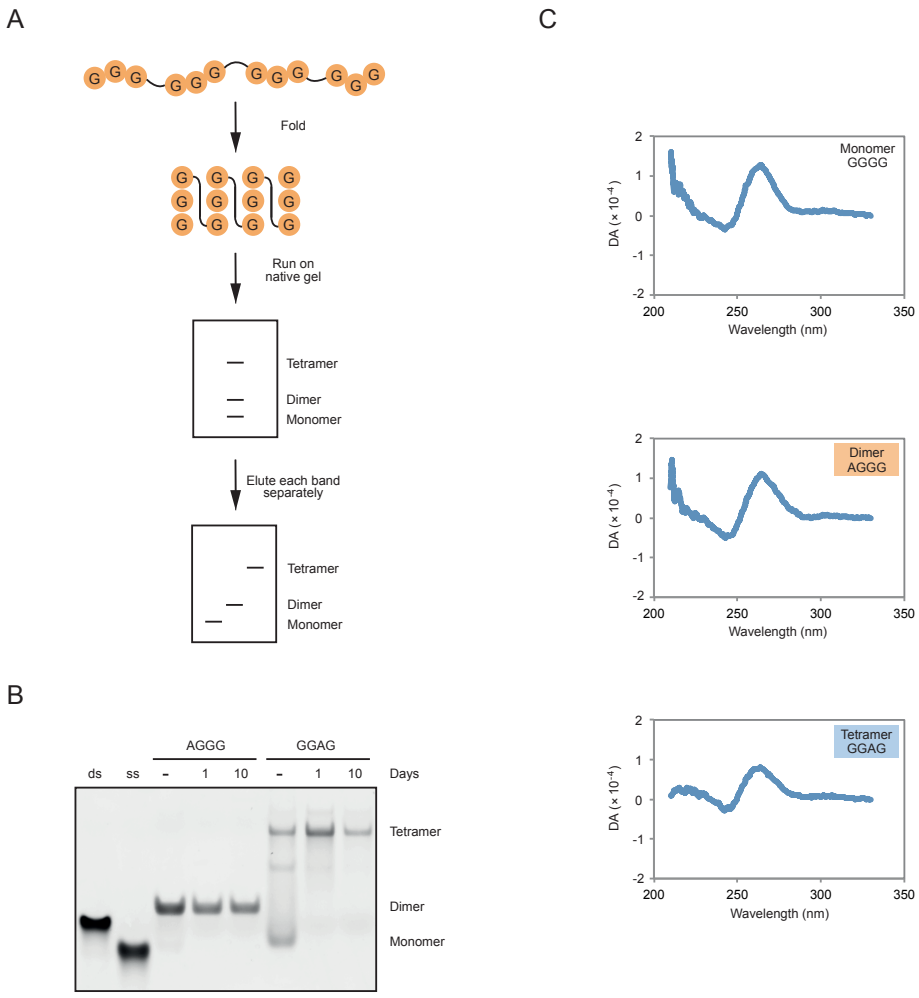

Supplementary Figure 6. Stability of gel-purified dimeric and tetrameric G-quadruplex structures. (A) Overview of method used to purify dimeric and tetrameric G-quadruplexes on native gels. (B) Native gel showing the stability of a gel-purified dimer and tetramer after 1 and 10 days. Lanes labeled with a dash contain DNA that was not gel purified. DNA was incubated for 30 minutes at room temperature at a concentration of 10 μM, and afterwards purified on a 10% native PAGE gel run in TBE buffer containing 5 mM KCl at 300 V for 30 minutes. After eluting into folding buffer (200 mM KCl, 1 mM $MgCl_2$, and 20 mM HEPES pH 7.1), DNA was incubated for either 1 or 10 days at room temperature and analyzed on a native gel stained with GelRed. (C) Circular dichroism spectra of a gel-purified monomer, dimer, and tetramer. Monomers were generated using a construct with a central GGGG tetrad with the sequence GGGTGGGAAGGGTGGGA. Dimers were generated using a construct with an AGGG mutation in the central tetrad of the reference construct and the sequence GAGTGGGAAGGGTGGGA. Tetramers were generated using a construct with a GGAG mutation in the central tetrad of the reference construct and the sequence GGGTGGGAAGAGTGGGA.

Supplementary Figure 7

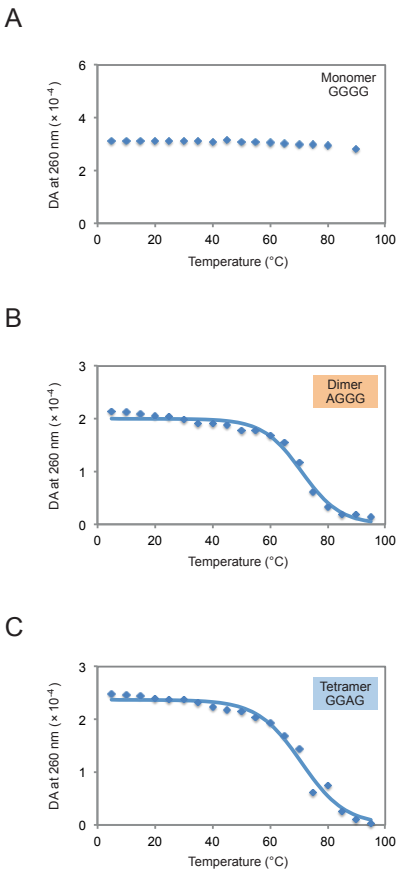

Supplementary Figure 7. Analysis of the thermal stability of monomeric, dimeric, and tetrameric G-quadruplexes by circular dichroism. (A) Differential absorption at 260 nm of a monomeric G-quadruplex with a central GGGG tetrad and the sequence GGGTGGGAAGGGTGGGA (*Tm* > 90°C). (B) Differential absorption at 260 nm of a dimeric G-quadruplex with an AGGG mutation in the central tetrad of the reference construct and the sequence GAGTGGGAAGGGTGGGA (*Tm* = 71°C). (C) Differential absorption at 260 nm of a tetrameric G-quadruplex with a GGAG mutation in the central tetrad of the reference construct and the sequence GGGTGGGAAGAGTGGGA (*Tm* = 71°C). All measurements were made in a buffer containing 200 mM KCl, 1 mM $MgCl_2$, and 20 mM HEPES pH 7.1. Curves were fit using the equation $DA = a / (1 + e^{(-(T-Tm)/b)})$, where DA is the differential absorption at 260 nm, T is the temperature, *Tm* is the melting temperature, and a and b are constants.

Supplementary Figure 8

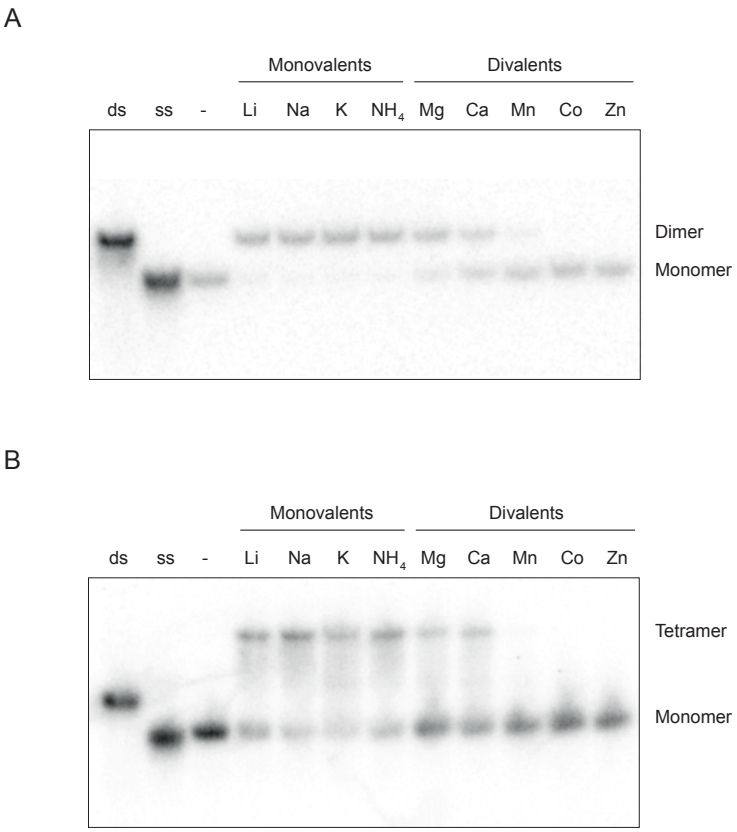

Supplementary Figure 8. Metal ion requirements of dimeric and tetrameric G-quadruplexes. (A) Native gel showing dimer formation in the presence of various monovalent and divalent metal ions. (B) Native gel showing tetramer formation in the presence of various monovalent and divalent metal ions. Experiments were performed at 1 μM G-quadruplex concentration in a buffer containing either 200 mM monovalent metal ion (LiCl, NaCl, KCl or NH_4Cl) and 20 mM HEPES pH 7.1 or 2 mM divalent metal ion ($MgCl_2$, $CaCl_2$, $MnCl_2$, $CoCl_2$ or $ZnCl_2$) and 20 mM HEPES pH 7.1. Experiments in panel A used a construct with an AGGG mutation in the central tetrad of the reference construct and the sequence GAGTGGGAAGGGTGGGA, and experiments in panel B used a construct with a GGAG mutation in the central tetrad of the reference construct and the sequence GGGTGGGAAGAGTGGGA.

Supplementary Figure 9

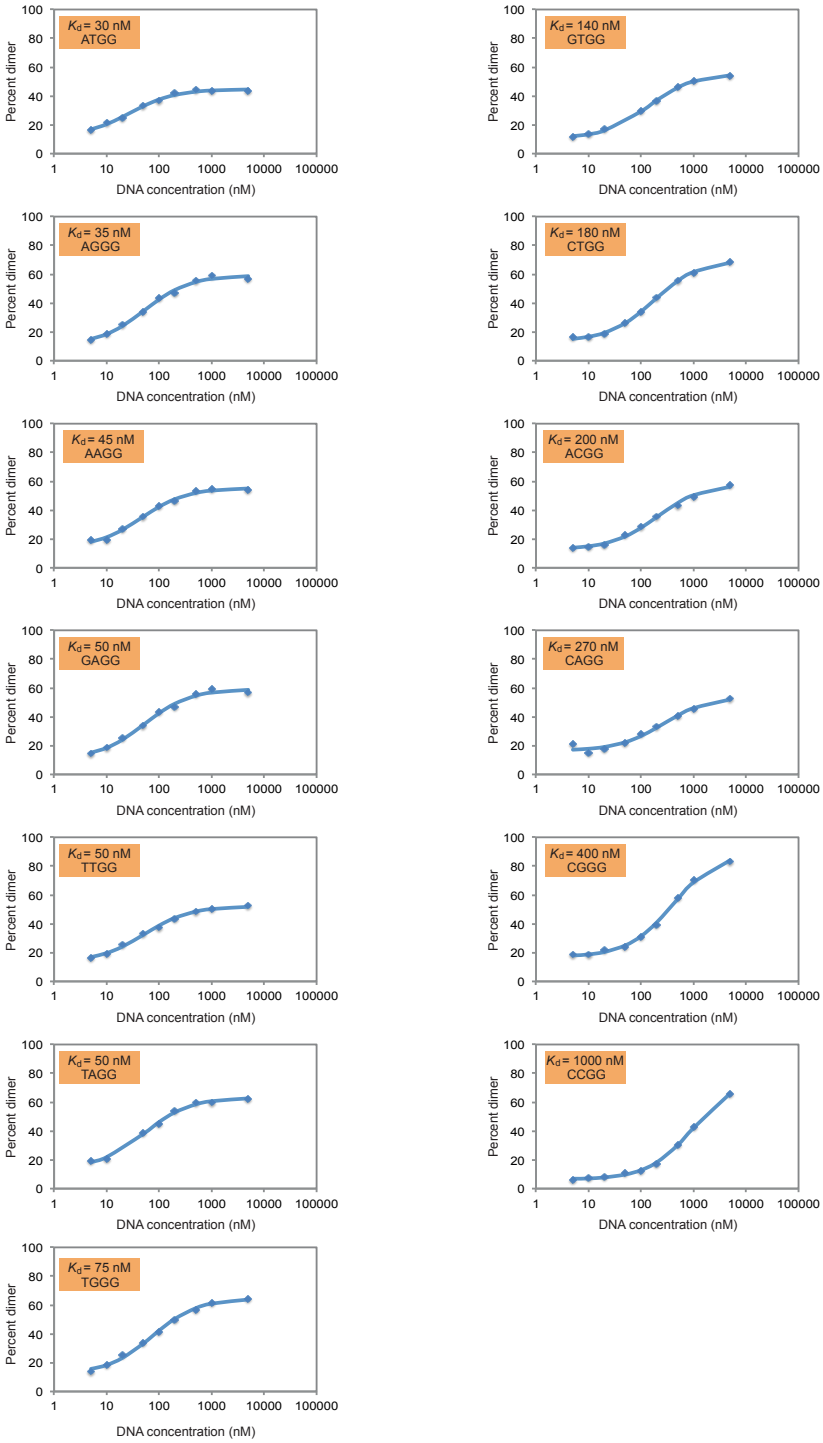

Supplementary Figure 9. Dimer formation as a function of DNA concentration for 13 of the mutants identified in our screen. Experiments were typically performed between 5 nM and 10 μM G-quadruplex concentration in a buffer containing 200 mM KCl, 1 mM $MgCl_2$, and 20 mM HEPES pH 7.1. K_d = the apparent dissociation constant of dimer formation.

Supplementary Figure 10

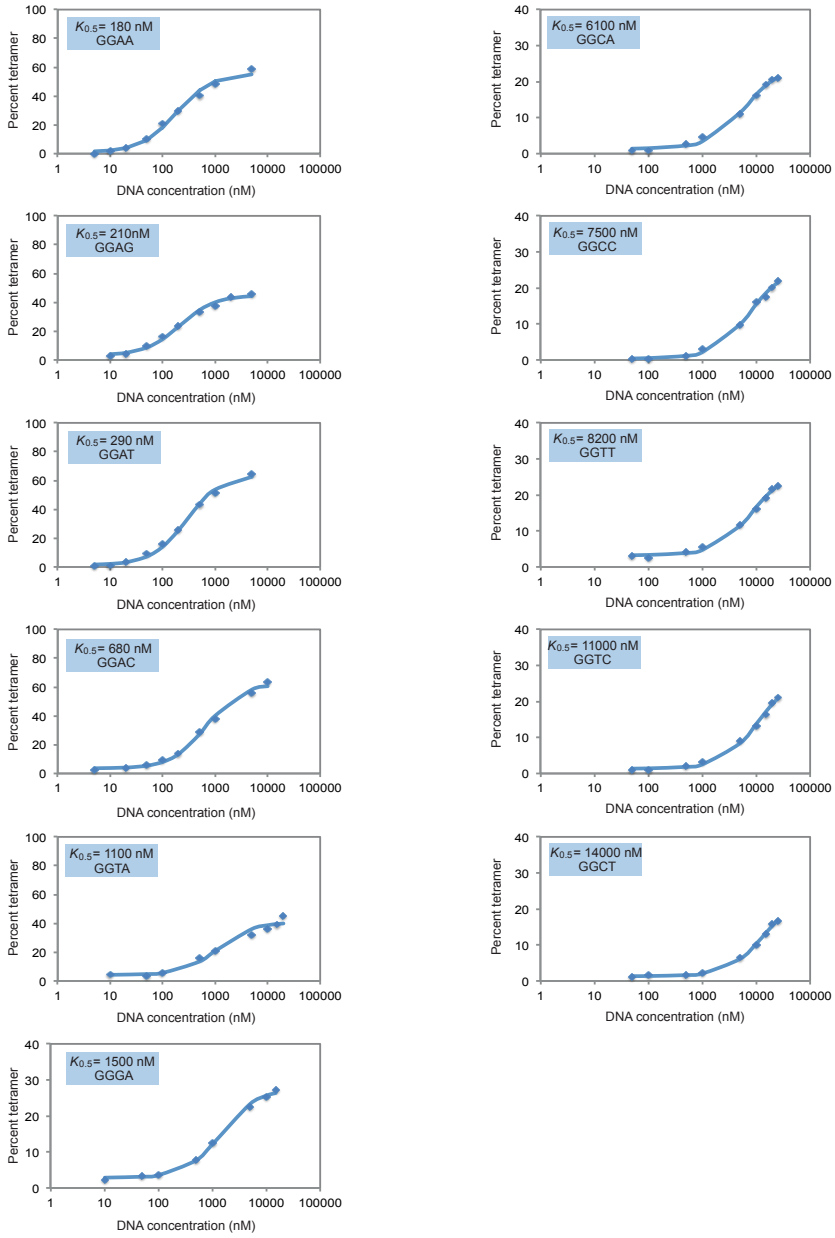

Supplementary Figure 10. Tetramer formation as a function of DNA concentration for 11 of the mutants identified in our screen. Experiments were typically performed between 5 nM and 50 μM G-quadruplex concentration in a buffer containing 200 mM KCl, 1 mM $MgCl_2$, and 20 mM HEPES pH 7.1. $K_{0.5}$ = the DNA concentration at which tetramer formation is half the maximum value.

Supplementary Figure 11

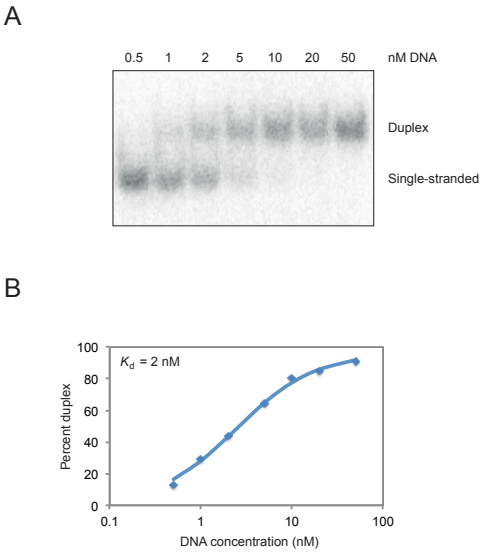

Supplementary Figure 11. Dissociation constant of a duplex formed by two complementary 17 nucleotide DNA strands. (A) Native gel showing duplex formation between a 17 nucleotide DNA oligonucleotide with the sequence GACTGCCTCGTCACGAT and its reverse complement. (B) Graph showing duplex formation as a function of DNA concentration. Experiments were performed between 0.5 nM and 50 nM DNA concentration in a buffer containing 200 mM KCl, 1 mM $MgCl_2$, and 20 mM HEPES pH 7.1. K_d = the apparent dissociation constant of duplex formation.

Supplementary Figure 12

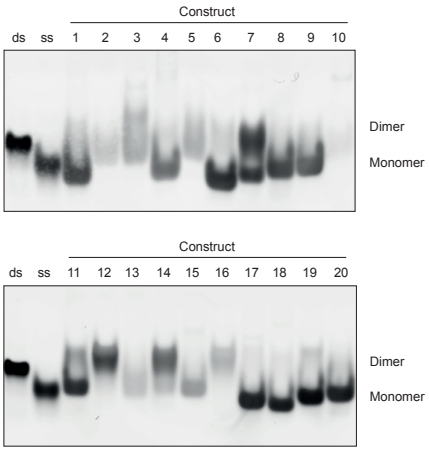

Supplementary Figure 12. Native gel showing the ability of twenty randomly chosen sequences consistent with an expanded sequence model to form dimers. This model allows sequences to contain a single mutated tetrad consistent with the sequence requirements described in Figure 6, and up to five mutations to occur in loops. Products were visualized by GelRed staining. Experiments were performed at 10 μM DNA concentration in a buffer containing 200 mM KCl, 1 mM $MgCl_2$, and 20 mM HEPES pH 7.1.

Supplementary Figure 13

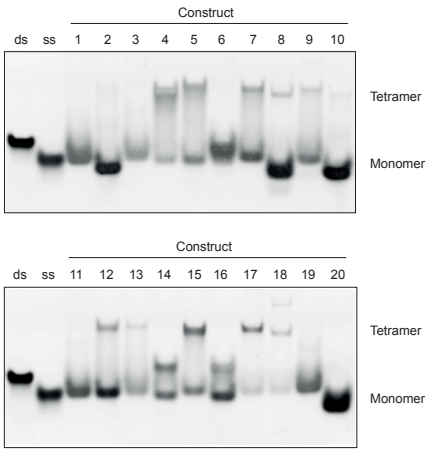

Supplementary Figure 13. Native gel showing the ability of twenty randomly chosen sequences consistent with an expanded sequence model to form tetramers. This model allows sequences to contain a single mutated tetrad consistent with the sequence requirements described in Figure 7, and up to five mutations to occur in loops. Products were visualized by GelRed staining. Experiments were performed at 10 μM DNA concentration in a buffer containing 200 mM KCl, 1 mM $MgCl_2$, and 20 mM HEPES pH 7.1.

Supplementary Figure 14

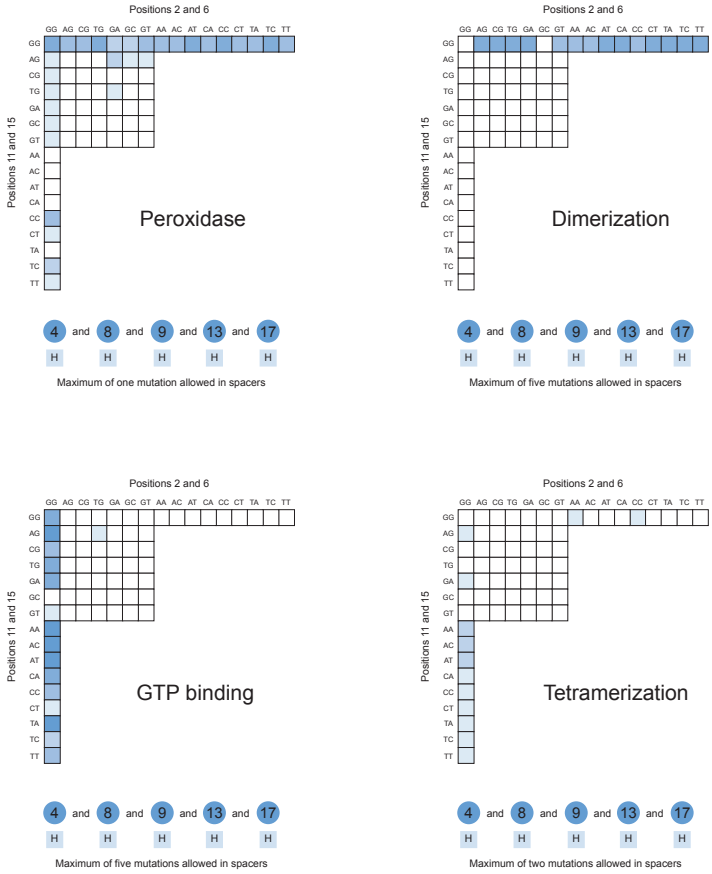

Supplementary Figure 14. Biochemical specificities of G-quadruplex variants with mutated central tetrads and mutated loops. In each heat map, darker blue represents higher biochemical activity. For simplicity only single and double mutant variants of the reference sequence are shown. GTP-binding and peroxidase activities are from Tables 1 and 2 of Švehlová et al. 2016 (reference 28 in the manuscript), and are expressed relative to the activity of a construct with a central GGGG tetrad. H = A, C, or T.

Supplementary Figure 15

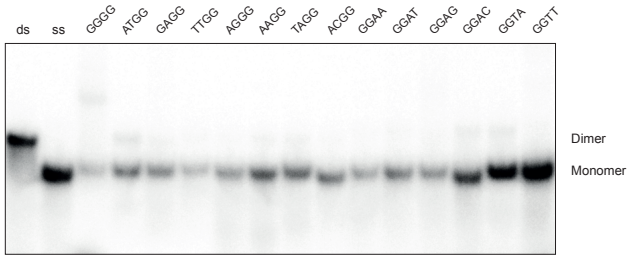

Supplementary Figure 15. Radiolabeled G-quadruplex variants exist primarily as monomers at the concentrations used in our screen for heteromultimer formation. Experiments were performed at ≤ 10 nM radiolabeled DNA concentration in a buffer containing 200 mM KCl, 1 mM $MgCl_2$, and 20 mM HEPES pH 7.1, and products analyzed on native gels.

Supplementary Figure 16

Positions mutated	Consecutive GGGG tetrads	Structure
2 and 6	4	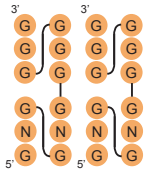
11 and 15	4	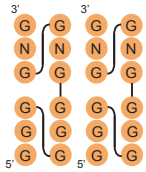
2 and 11	2	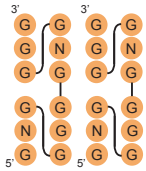
2 and 15	2	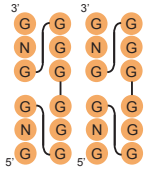
6 and 11	2	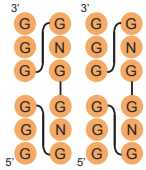
6 and 15	2	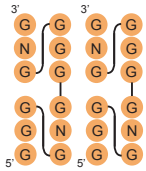

Supplementary Figure 16. Effects of mutations at all possible pairs of positions in the central tetrad of the reference G-quadruplex on the number of consecutive GGGG tetrads in an intertwined dimer.

Supplementary Figure 17

Positions mutated	Consecutive GGGG tetrads at interface	Structure
11 and 15	8	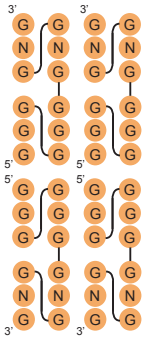
2 and 6	2	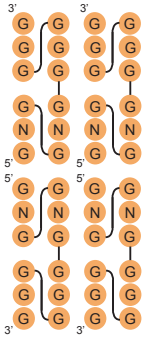

Supplementary Figure 17. Effects of pairs of mutations at positions 2 and 6 or 11 and 15 on the number of consecutive GGGG tetrads flanking the interface in a tetramer formed from two 5'-5' stacked intertwined dimers.

Supplementary Figure 18

Composition of tetramer	Consecutive GGGG tetrads at interface	Structure
4 GGNN 0 NNGG	8	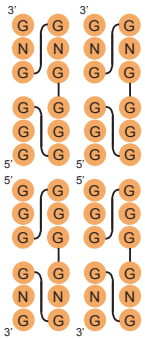
3 GGNN 1 NNGG	5	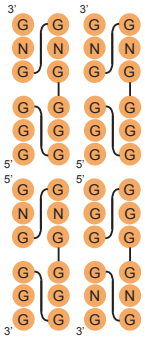
2 GGNN 2 NNGG	5	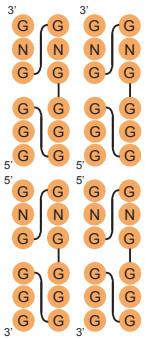

Composition of tetramer	Consecutive GGGG tetrads at interface	Structure
2 GGNN 2 NNGG	2	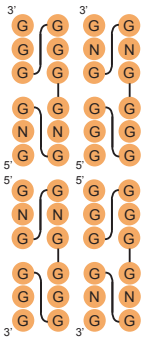
1 GGNN 3 NNGG	2	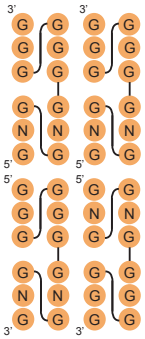
0 GGNN 4 NNGG	2	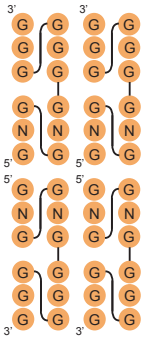

Supplementary Figure 18. Expected number of consecutive GGGG tetrads flanking the interface in tetramers formed from different ratios of molecules with mutations at 2 and 6 (NNGG) or 11 and 15 (GGNN).

Figure	Name	Sequence
6C	Construct 1	GAGTGGGTAGGGCGGGT
	Construct 2	GAGAGGGTTGGGTGGGT
	Construct 3	GAGAGGGTTGGGCGGGC
	Construct 4	GAGTGGGACGGGCGGGT
	Construct 5	GAGCGGGAAGGGCGGGA
	Construct 6	GAGCGGGAAGGGAGGGC
	Construct 7	GAGCGGGTTGGGCGGGC
	Construct 8	GAGAGGGACGGGCGGGC
	Construct 9	GAGAGGGTCGGGTGGGC
	Construct 10	GAGCGGGTAGGGTGGGC
7C	Construct 1	GGGCGGGCAGAGTGGGA
	Construct 2	GGGTGGGATGAGTGGGC
	Construct 3	GGGTGGGATGAGCGGGA
	Construct 4	GGGTGGGACGAGAGGGA
	Construct 5	GGGCGGGTAGAGTGGGA
	Construct 6	GGGTGGGACGAGTGGGC
	Construct 7	GGGTGGGACGAGTGGGT
	Construct 8	GGGTGGGTAGAGCGGGA
	Construct 9	GGGTGGGTAGAGAGGGA
	Construct 10	GGGTGGGTAGAGTGGGC

Supplementary Table 1. Sequences of constructs tested for dimer and tetramer formation that contain multiple mutations in loops.